Stability and structure of rare-earth metal and Ba-induced reconstructions on a Si(100) surface

M. P. J. Punkkinen,[1,2,*] M. Kuzmin,[2,3] P. Laukkanen,[2,4] R. E. Perälä,[2] M. Ahola-Tuomi,[2] J. Lång,[2] M. Ropo,[5] M. Pessa,[4] I. J. Väyrynen,[2] K. Kokko,[2] B. Johansson,[1,6] and L. Vitos[1,6,7]

[1]*Applied Materials Physics, Department of Materials Science and Engineering, Royal Institute of Technology, SE-10044 Stockholm, Sweden*

[2]*Department of Physics and Astronomy, University of Turku, FI-20014 Turku, Finland*

[3]*A. F. Ioffe Physico-Technical Institute, Russian Academy of Sciences, St. Petersburg 194021, Russian Federation*

[4]*Optoelectronics Research Centre, Tampere University of Technology, FI-33101 Tampere, Finland*

[5]*Department of Information Technology, Åbo Akademi University, FI-20500 Turku, Finland*

[6]*Condensed Matter Theory Group, Physics Department, Uppsala University, SE-75121 Uppsala, Sweden*

[7]*Research Institute for Solid State Physics and Optics, P.O. Box 49, H-1525 Budapest, Hungary*

(Received 21 May 2009; revised manuscript received 26 October 2009; published 4 December 2009)

We have studied, by means of *ab initio* calculations, the energetics and the atomic and electronic structures of various reconstructions induced by rare-earth metals (RE=Eu, Nd, Sm, and Yb) and Ba on Si(100) in the coverage range up to 0.5 monolayer. It is shown that Si dimer buckling is an important structural element for such systems, leading frequently to oblique surface lattice symmetries. The strong metal atom—silicon binding favors the increased amount of metal atoms per unit surface area, i.e., the (2×3) reconstruction with two metal atoms per unit cell is found to be energetically unstable with respect to the (2×1) reconstruction with three metal atoms per the same surface area [Eu/Si(100) and Yb/Si(100)]. The influence of the atomic size and the valence of the adsorbates is also investigated. In particular, it is found that an increase in atomic size stimulates the metal-metal repulsion, stabilizing the (2×3) configuration [Ba/Si(100)]. In the case of trivalent metals, the stabilization of the (2×3) is mediated by the loss of semiconducting state in the competing phases [Sm/Si(100) and Nd/Si(100)]. Our results demonstrate the importance of many factors, which account for the abundance of RE/Si(100) reconstructions. Finally, prominent atomic models are proposed for (2×3) and (2×6) reconstructions, and the character of the wavy "(1×2)" reconstruction is discussed. The simulated scanning tunneling microscopy images for the proposed (2×6) reconstruction are in a particularly good agreement with the complex experimental images.

DOI: 10.1103/PhysRevB.80.235307 PACS number(s): 68.43.Bc, 68.35.bg, 68.37.Ef

I. INTRODUCTION

Metals on silicon produce a variety of surface reconstructions with diverse atomic and electronic structures. Understanding these structures and the mechanisms controlling the stability of such interfaces has been a long-term purpose in semiconductor surface studies. Among the metal/Si reconstructions, the widespread and frequently experimentally found (2×3) phase formed by numerous metals on Si(100) in the submonolayer coverage regime [$\leq 1/3$ monolayer (ML)] has attracted much interest because it can serve as a prototype reconstruction.[1] Different structural models have been proposed for metal/Si(100)(2×3). In earlier work, the metal atoms were assumed to reside at specific adsorption sites in the dimer row (2×1) reconstruction of the clean Si(100).[2] Later on, scanning tunneling microscopy (STM) evidenced that the Si substrate can be rearranged by metal atoms. For example, the model proposed for Na/Si(100)(2×3) suggests the top Si-atom density of 1/3 ML and includes alternating dimeric and monomeric Si rows.[3] Similar, albeit not equivalent, rearranged Si structures have been considered for Ba (Refs. 4–6) and Eu.[1] Theoretical support, however, has been so far very rare for these models, Ba/Si(100) (Ref. 7) being one exception.

Recently, we employed first-principles calculations and core-level spectroscopy to elucidate the atomic geometry of Yb/Si(100)(2×3) and (2×4) phases in detail.[8] Based on total-energy calculations, favorable structures have been reported, where the Yb atoms are completely divalent ($4f^{14}6s^2$) and have the 1/3 and 3/8 ML coverages, respectively. The first-layer Si atoms of these phases have a tendency to dimerize, although the fully optimized atomic configurations are different from that of the clean substrate. Europium ($4f^76s^2$) is very similar to Yb electronically, and Eu/Si(100)(2×3) and Yb/Si(100)(2×3) are isoelectronic systems. Significant difference between Eu and Yb, however, can originate from their different local magnetic moments and therefore, it is interesting to compare results for Eu/Si(100) and Yb/Si(100). Both surfaces show the (2×3) reconstruction but only the latter does the (2×4).

In this study we investigate, by various theoretical methods and approximations, the above and other reconstructions induced by different metals on Si(100) in the coverage range up to 1/2 ML [(2×1), (2×6), and the so-called wavy "(1×2)" phases]. In particular, it is shown that the (2×1) reconstruction is energetically favorable and our calculations predict it to be more stable than the (2×3) reconstruction of the Eu/Si and Yb/Si, found in experiment, regardless of the chemical potential of Eu or Yb. We note that in the following we mean by (2×3) reconstruction a structure with two metal atoms per (2×3) surface area, if not stated otherwise [other possibility is one metal atom per (2×3) surface area]. In order to realize this finding, we examine different factors behind the relative stabilities. Especially it is found that the buckling of Si dimers lowers the energy of the Eu/Si(100)

and Yb/Si(100) surfaces. Furthermore, to understand the role of atomic properties and electronic configuration of the adsorbate atoms, other representative metals (Ba, Sm, and Nd) on Si(100) are considered. Similar to Eu and Yb, barium is divalent; it differs from these RE metals only by the nonexistence of the 4*f* electronic shell. Contrary to these divalent metals, Nd is a typical trivalent RE element while Sm can readily change the valence between the divalent and trivalent states depending on the surrounding and have an intermediate valence. Therefore, a comparative study of Eu, Yb, Ba, Nd, and Sm/Si(100) reconstructions can elucidate the impact of the atomic and electronic properties of the adsorbates on the stability and structure of these systems. Finally, we propose prominent atomic models for the (2×3) and (2×6) reconstructions as well as discuss the geometry and formation mechanism of the wavy (1×2) reconstruction.

The rest of the paper is organized as follows: in Sec. II the calculational methods are described. Results are presented and discussed in Sec. III: Sec. III A introduces the Si dimer buckling to the RE/Si(100) reconstructions, Sec. III B presents results obtained by different approximations to shed light on the energy difference between the (2×1) and (2×3) reconstructions, Sec. III C describes the effect of atom size and valence on the relative stabilities, and the Sec. III D considers reconstructions found experimentally around 1/2 ML. The paper ends with conclusions.

II. CALCULATIONAL METHODS

Calculations were performed using an *ab initio* density-functional total-energy method within the local-density approximation (LDA).[9,10] The approach is based on plane-wave basis and projector augmented wave method[11,12] (Vienna *ab initio* simulation package).[13–16] The optimization of the atomic structure was performed using conjugate-gradient minimization of the total energy with respect to the atomic coordinates. Slabs with 12 atomic layers (one metal-atom layer and 11 Si layers) were used. The dangling bonds of the bottom surface Si atoms were passivated by hydrogen atoms. For Ba, Eu, and Yb, the *f* electrons were treated as core electrons in most of the calculations, whereas for Sm and Nd one *f* electron was in the valence, which leads to trivalency in accordance with experiment. Two bottom atomic layers of the slabs were fixed to the ideal positions. Other atoms, including hydrogen atoms, were relaxed until the remaining forces were less than 20 meV/Å. The number of *k* points in the Brillouin zone was equivalent to 144 *k* points in the Brillouin zone of the (1×1) slab. Some calculations were repeated with a *k* mesh equivalent to 576 *k* points per (1×1) surface unit cell. The larger amount of *k* points led only to marginal changes in results. The *k*-point sampling was performed by the Monkhorst-Pack scheme[17] with the origin shifted to the Γ point. The plane-wave cutoff energy was 280 eV. The relative surface energies were evaluated as a function of chemical potentials of the surface constituents $(\mu_{\mathrm{RE}},\mu_{\mathrm{Si}})$ by

$$\gamma A = E_{\mathrm{tot}} - n_{\mathrm{RE}}\mu_{\mathrm{RE}} - n_{\mathrm{Si}}\mu_{\mathrm{Si}} \quad (1)$$

in which n_i denotes the number of atoms of type *i* in the unit cell and the E_{tot} is the total energy of the unit cell. In practice, only the contribution from the RE atoms was subtracted in most of the cases. The contribution from the third term on the right side of Eq. (1) was included only when the first Si layer was not completely filled. Because the reconstructions studied have different dimensions of unit cells, the surface energy for each individual reconstruction was compared also to that of a reference system [in this case the (2×1) reconstruction]. The lattice parameter of the cubic unit cell of the bulk diamond structure (*a*) was fixed to our calculated value of 5.40 Å. Thus, the surface lattice parameter is 3.82 Å ($a_S=a/\sqrt{2}$). The constant-current STM images were simulated within the Tersoff-Hamann approximation.[18]

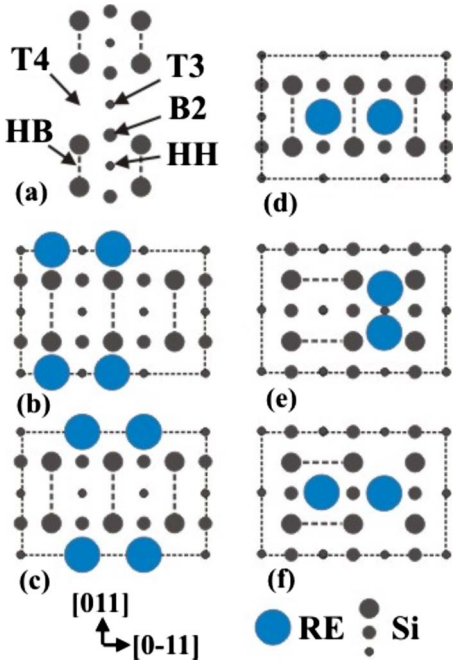

FIG. 1. (Color online) (a) Adsorption sites on Si(100) with first layer Si dimers. [(b)–(f)] Structural models of the (2×3) reconstruction. The dashed line boxes represent (2×3) unit cells and the gray dashed lines the orientation and position of the first-layer silicon dimers.

III. RESULTS AND DISCUSSION

A. Eu/Si(100)(2×3) and Yb/Si(100)(2×3): Buckled Si dimers

First, we consider (2×3) reconstructions of Eu and Yb on Si(100). In examined models, the metal coverage is 1/3 ML [i.e., the (2×3) unit cell includes two RE atoms] and the buckled first layer Si dimers are initially removed. However, the bulk-terminated Si structure is energetically unstable and therefore, we allow the first-layer Si atoms to move slightly from their positions on Si(100)(1×1) to dimerize. The most favorable adsorption sites on such a surface are T3 (valley bridge) and T4 (cave), whereas HH (pedestal), HB (dimer bridge), and B2 (intermediate bridge) are less preferable [Fig. 1(a)].[19] Hence, we assume the RE atoms to reside initially at either T4 or T3 [Figs. 1(b) and 1(c), respectively]. Similar models were considered for Yb/Si(100)-(2×3) in Ref. 8 [the initial (2×3)-I and (2×3)-II structures]. In ad-

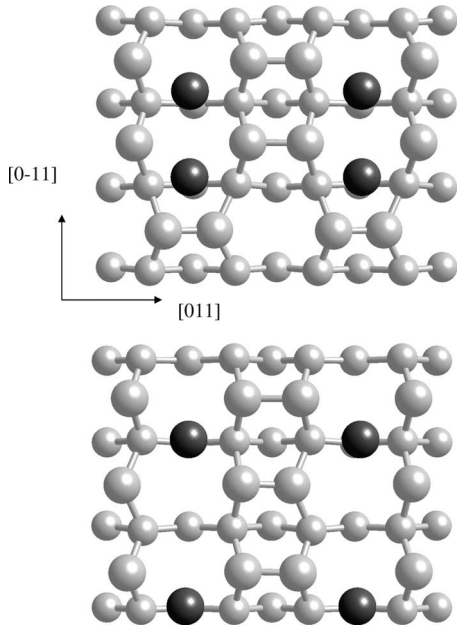

FIG. 2. Surface atomic structures (top view) of (2×3)-I (top panel) and (2×3)-II (bottom panel) reconstructions on Eu/Si(100). The (2×3)-II has a more symmetrical pattern of Si dimers. The black spheres denote Eu atoms and the gray spheres denote Si atoms. Atoms in the first and second layers are shown by larger spheres.

dition, we tested a model with a less stable site (HH) shown in Fig. 1(d) and the models proposed earlier for Ba (Ref. 6) and Eu (Ref. 1) [Figs. 1(e) and 1(f), respectively].

Our calculations indicate that the models in Figs. 1(e) and 1(f) are very unstable and that the energies of such structures after their full optimization are higher by ~1 eV per (2×3) slab than those of Figs. 1(b) and 1(c). Therefore, we reject the models based on the dimeric and monomeric Si rows for RE/Si(100)-(2×3). This is easily understood because the number of Si dangling bonds in these models is higher. Dimerization of Si atoms decreases the total energy considerably.

The optimization of the models in Figs. 1(b)–1(d) reveals that the fully relaxed structure corresponds to the model with the T3 adsorption site [Fig. 1(c)]. In other words, the metal atoms locate always on the valley-bridge adsorption sites. However, one can find two different patterns of first-layer Si dimers as in our previous work for Yb/Si(100). One of the patterns [(2×3)-II] is more symmetrical than the other [(2×3)-I]. Moreover, our finding reveals that one of the three first-layer Si dimers in both reconstructions both for Yb/Si(100) and Eu/Si(100) is buckled. The corresponding surface structures are shown in Figs. 2 and 3. If there was no buckling, then the ground state for Yb/Si(100) would be (2×3)-I (as was stated in our previous work) while the ground state for Eu/Si(100) would be (2×3)-II. Interestingly, the stability of the (2×3)-I increases relative to the (2×3)-II as the volume of the substrate increases. Conversely, this means that the stability of the (2×3)-I increases as the size of the adsorbed metal atom decreases, which is our observation (volume of the Yb atom is smaller than that of the Eu atom). However, the buckling of one of the

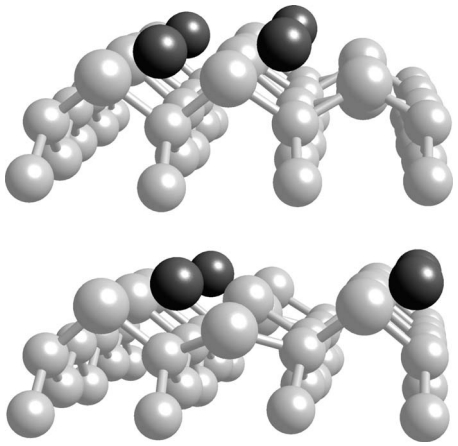

FIG. 3. Surface atomic structures of (2×3)-I and (2×3)-II Eu/Si(100) reconstructions (side view). The black spheres denote Eu atoms and the gray spheres denote Si atoms. Atoms in the first and second layers are shown by larger spheres.

first-layer Si dimers decreases total energy on both surfaces and makes the (2×3)-II stable for both Yb/Si(100) and Eu/Si(100) surfaces. Therefore, the ground-state reconstruction involves the symmetrical pattern of first-layer Si dimers and buckling. The buckling decreases total energy by 0.015 eV/(1×1) area for the Eu/Si(100) and 0.033 eV/(1×1) area for the Yb/Si(100). Moreover, the additional lowering of the surface energy can be achieved by a symmetry change from the rectangular lattice to an oblique one, which leads to a further decrease in energy by 9 meV/(1×1) area for the Eu/Si and 3 meV/(1×1) area for the Yb/Si. Then, the surface lattice vectors are $(2a_S, a_S)$ and $(0, 3a_S)$. This symmetry change enhances the buckling of the Si dimers; the buckled dimers are tilted by 0.68–0.71 Å for the oblique lattice and 0.54–0.56 Å for the rectangular lattice. The dimer tilting in the oblique case is comparable to that of the pure Si(100) surface (0.78 Å). Note that a slight tilt (0.15–0.16 Å for the second Si dimer in the oblique case and smaller than 0.1 Å for the third one and rectangular case) is also found for the other two ("unbuckled") dimers. Furthermore, the RE atoms are shifted in the direction perpendicular to the direction of RE atom pair slightly more away from each other in the oblique structure. Such tendency to the oblique symmetry is found, e.g., in the experimental STM images for the Yb/Si(100) in Figs. 5(c) and 5(d) in Ref. 20.

It is worth to note that the (2×3) surface is semiconducting irrespective of the amount of adsorbed atoms in the (2×3) mesh (0, 1, 2, or 3) up to 1/2 MLs. This is understood, when we think the situation in the spirit of the electron counting model[21] [or generalized electron counting model (Refs. 22 and 23)]. For Si(100)(2×1), the dangling-bond states related to the lower and upper atoms of the buckled Si dimer lie in the conduction and valence bands, respectively,[24] and thus the dangling bond of the lower atom is empty and that of the upper atom is filled. This is a reminiscence of the polar III-V(100) surface, where the group III atom is a cation and the group V atom is an anion. Within this picture one can easily see that there are many ways to keep the Eu and Yb/

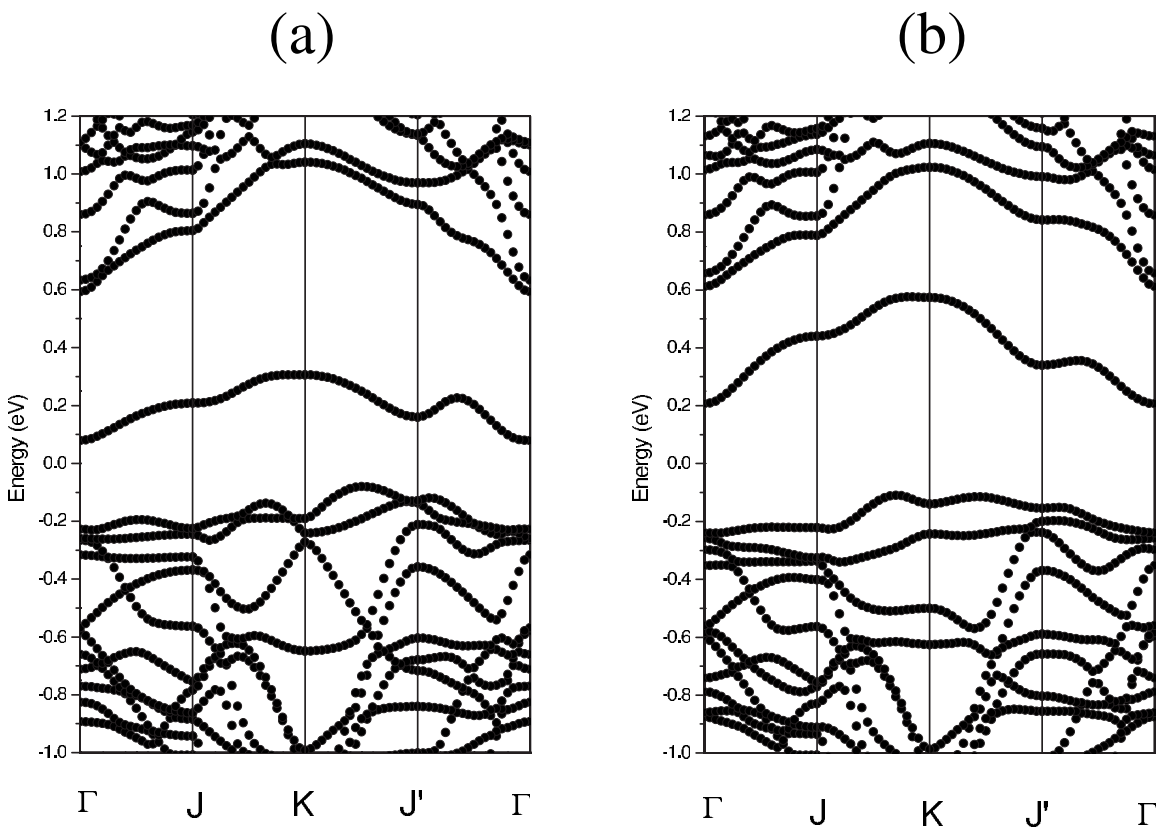

FIG. 4. Band structures of Eu/Si(100)(2×3) (a) with no buckled dimers and (b) with one buckled dimer per (2×3) unit along high-symmetry directions.

Si(100) surfaces semiconducting due to the divalency of the RE atoms and the inequivalency of dimers. If there is a single divalent RE atom per (2×3) area (coverage of 1/6 ML), it can donate two electrons to Si dimers. Then, one of the Si dimers donates two electrons to other two Si dimers, of which both dangling bonds become occupied. It is also possible that two Si dimers become buckled and then, the metal atom donates two electrons for the third Si dimer. If there are two metal atoms per (2×3) area (the 1/3 ML coverage), two scenarios are also possible. If only one metal atom donates its electrons, all the dimers can be unbuckled. But they are not equivalent (one of them locates in a different vertical position). It is energetically more favorable, however, that four electrons are donated from both metal atoms, which leads to one buckled dimer. Finally, if there are three metal atoms (the 1/2 ML coverage), then each of the metal atoms donates two electrons to one Si dimer, leading to a (2×1) structure. Figure 4 shows the band structures calculated for the Eu/Si(100)(2×3) at 1/3 ML for the cases, where there are no buckled dimers and where there is one buckled dimer. Inspection of band characters reveals that in the buckled case there is indeed a considerable contribution to the highest occupied band from the upper Si dimer atom and to the lowest unoccupied band from the lower Si dimer atom. In the unbuckled case there is a significant contribution to the lowest unoccupied band from the Si dimer, which is closer to bulk (than the other two Si dimers). One can note that in symmetry directions J-K and K-J′ some bands become considerably less dispersive, when one Si dimer is buckled. The character of these band changes upon buckling from quite delocalized to more localized. In the latter case these bands originate mainly from the upper buckled dimer atom (which has more electronic charge than the lower buckled dimer atom) and the near metal atom indicating stronger covalent bonding compared to the unbuckled case. Thus, the above modification of the electronic structure is consistent with the fact that the buckling of Si dimers is energetically favorable. The similar results are also found for the oblique lattice.

B. Remarkable stability of the (2×1) reconstruction

The finding of the prevalence of the semiconducting state irrespective of the amount of metal atoms led originally us to compare the relative energies of the surfaces with different metal coverages. It is surprising that the (2×3) reconstruction at 1/3 ML [two metal atoms in the (2×3) unit] is not stable theoretically at all irrespective of the value of the chemical potential for the Eu or Yb atom. The results for the Yb/Si(100) are shown in Fig. 5(a) and for the Eu/Si(100) in Fig. 5(b) [in which also other reconstructions (see Sec. III D) are shown]. As seen, the ground state for the Eu/Si is the (2×1) structure and this structure is more stable than the (2×3) also for the Yb/Si. Note that such a structure has been experimentally found for neither Yb nor Eu. The theoretical STM images for the Eu-induced (2×1) and (2×3) reconstructions with buckled Si dimers are shown in Fig. 6. The images for the (2×3) reconstruction are in reasonable agree-

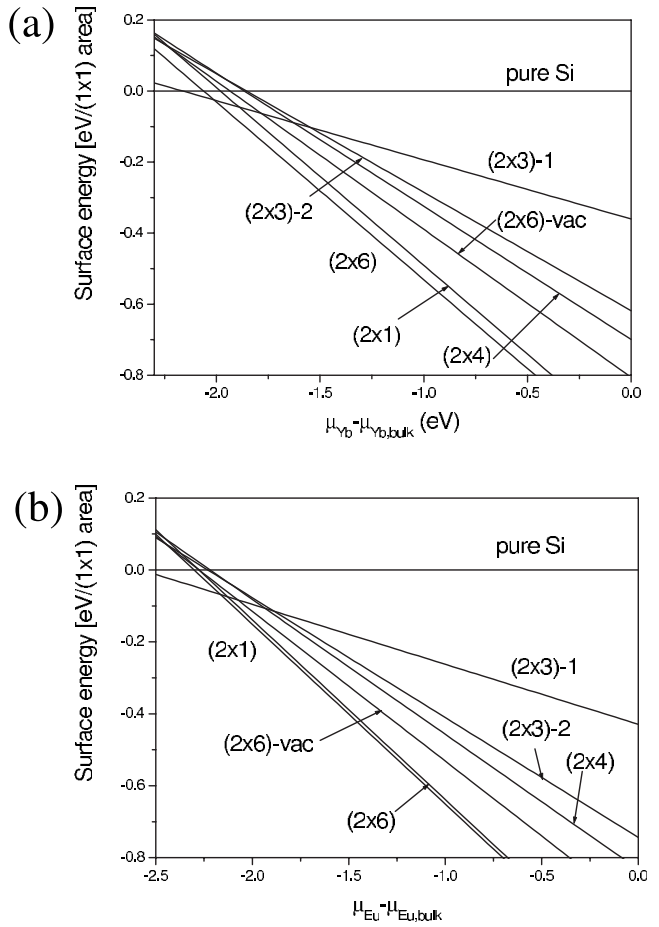

FIG. 5. Surface phase diagrams for (a) Yb/Si(100) and (b) Eu/Si(100). The atomic model for the (2×4) reconstruction is the same as the ground-state atomic model in Ref. 8. The "(2×3)-1" means that there is one metal atom per (2×3) area (1/6 ML) and the "(2×3)-2" that there are two metal atoms per (2×3) area (1/3 ML). One should note that the interesting area is around the onset of the stability of pure Si(100) surface. When the chemical potential of bulk metal (right edge) is approached, other reconstructions not considered in this study are stabilized.

ment with the experimental STM images that showed the rows of paired protrusions.[1] (Note that experiments in room temperature might not discriminate between buckled and unbuckled cases.) Whereas the image for the (2×1) structure shows unresolved bright lines, which is fully inconsistent with the measured data. The total energy of the (2×3) reconstruction at 1/6 ML (one RE metal atom) is significantly decreased in the oblique symmetry [about 0.06 eV/(1×1) area], which is probably due to the buckling of two Si dimers. The buckling is about 0.12 Å for two Si dimers, whereas for the rectangular lattice the buckling is practically zero (on the order of 10^{-4} Å). It is interesting that the (2×3) with one metal atom is stable for all considered metal atoms. This suggests that if there are two metal atoms, then the energy decrease due to buckling is relatively smaller for the (2×3) than for the one atom case [for the (2×1) there is no buckling] and then it does not compensate the energy increase relative to the (2×1) reconstruction due to smaller amount of metal-silicon binding.

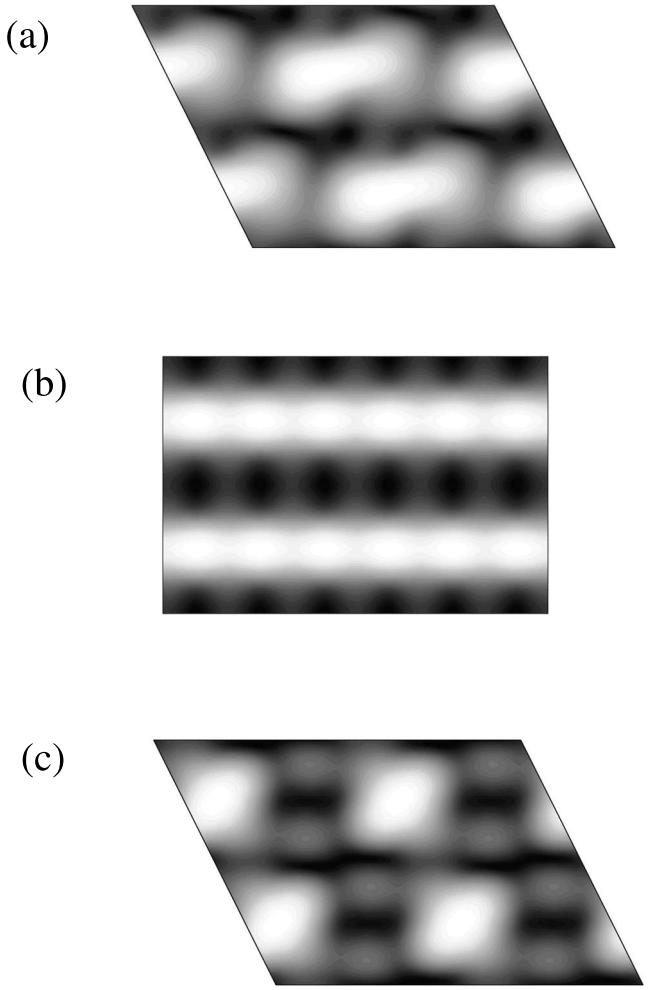

FIG. 6. Simulated STM images for the Eu/Si(100) (a) (2×3)-II structure (one buckled dimer, oblique lattice), (b) (2×1) structure, and (c) (2×3) structure with one Eu atom in the unit cell with energy range of 1.4 eV above the Fermi energy.

Since the RE atoms have generally an open f shell, it was investigated, whether the treatment of the f electrons can affect the results significantly. We had found that calculations are not easily converged for the Eu/Si(100), if the f electrons are treated as valence electrons. This is well understood because in case of Eu, there is a large density of states at the Fermi level within the LDA or local-spin-density approximation (LSDA). Therefore, we performed also LSDA+U calculations (rotationally invariant form of the functional,[25] $U=3-8$ eV). We found that the relative stabilities for both Eu/Si(100) and Yb/Si(100) are practically unchanged, whether or not the f electrons are treated as valence electrons, although the Eu atoms have significant magnetic moments, if the f electrons are valence electrons. Within the LSDA+U the energy difference between the (2×3) and (2×1) reconstructions is slightly changed but the relative stability remains the same as in the case of LDA calculations. The inclusion of the spin-orbit interaction does not change the relative stability either. One could still suspect that the correct (2×3) model has not been found. For this reason, the calculations were repeated by using (2×6), (4×3), and (4×6) surface cells to study, whether there could be a different

kind of pattern of buckled dimers. The calculations reveal that this is not case. The buckled dimers may buckle in opposite directions in neighboring (2×3) cells in the $[0\bar{1}1]$ direction in a (2×6) cell but this has a marginal effect on the total energy due to the large distance between buckled dimers. The metal atoms grouped in a pair were also put in different positions in the $[0\bar{1}1]$ direction in neighboring (2×3) cells in a (4×3) cell but this does not lead to a new total-energy minimum, not even in oblique symmetry, in which there is more freedom for buckled Si dimers to order or pattern in a (4×3) cell. The metal-atom pairs of the (2×3) reconstruction were also put alternatively on neighboring metal-atom rows, which did not decrease the total energy either. All these results suggest that the interaction between the metal-atom pairs is weak. We note also that using the GGA exchange-correlation energy functional did not lead to qualitative changes in results.[26] It is interesting that the surface phase diagrams are quite similar to both of Eu/Si(100) and Yb/Si(100), which suggests that magnetism does not affect these results noticeably because the magnetic moments of divalent Yb atoms are zero. The magnetism is vanished due to small number of magnetic neighbors.

It is possible that configurational entropy stabilizes the (2×3) reconstruction. In experiment, the samples were typically prepared at 530–600 °C. If configurational entropy is included according to the model in Ref. 27, then there is a larger probability for the (2×3) reconstruction than for the (2×1) reconstruction at 800–900 K for low values of $\mu_{\mathrm{Eu,Yb}}$ (probabilities are in relation of 5:4 at 900 K, respectively). In this model the statistical probability c_i of a particular reconstruction i is obtained as

$$Z_i = g_i \exp[-\gamma_i^0(\mu_{\mathrm{RE}},\mu_{\mathrm{Si}})A/k_BT], \tag{2}$$

$$Z = \sum_i Z_i, \tag{3}$$

$$c_i = Z_i/Z \tag{4}$$

in which the Z is the partition function, which is defined independently for each unit cell of area A, γ_i^0 is the surface energy at 0 K, and g_i is a symmetry-determined degeneracy factor. However, at room temperature, the probability of the (2×1) reconstruction is significantly higher than that of the (2×3) (probabilities are in relation of 5:1, respectively). Therefore, the stabilization of the (2×3), observed at this temperature after the annealing in experiment, should be both due to configurational entropy and kinetics. However, one could easily think that there are high diffusion barriers to prevent the transformation of the (2×3) reconstruction into combination of the (2×1) reconstruction and some other phase. Kinetics may contribute to the existence of the (2×3) reconstruction also at high temperatures because the (2×3) was mostly found around coverages of 1/3 ML, whereas the metal-atom coverage for the (2×1) reconstruction is 1/2 ML.

On the other hand, it is very well possible that some experimental findings for the (2×3) reconstruction are for the structure with one metal atom per (2×3) surface area, which is stable. Especially, because the STM images are rather similar for the reconstructions with one atom and two atoms [an STM image for the Eu/Si(100)(2×3) with one metal atom is shown in Fig. 6(c)]. The (2×3) with one metal atom was clearly found in Ref. 28.

C. Effect of the adsorbate size and valence on the relative stability

Next, some (2×3) reconstructions with different adsorbates are considered. The Ba/Si(100) surface was chosen because it has been investigated in numerous experimental studies and moreover it is divalent like Eu and Yb, as mentioned in Sec. I. Calculations were repeated also for other models shown in Fig. 1 to confirm that we use the correct energy for the (2×3) reconstruction. The calculations confirm that the (2×3)-II model (with a buckled dimer and oblique symmetry) is the stable one of the (2×3) models for the Ba/Si(100) as well [buckling decreases energy by 0.012 eV/(1×1) area and oblique symmetry also by 0.012 eV/(1×1) area]. This result is in agreement with the previous experimental[4,5] and theoretical results[7] but in a disagreement with the experimental results from Ref. 6. Interestingly, the relative stability of the (2×3) with respect to the (2×1) is higher for Ba than for Eu and Yb [Fig. 7(a)]. This is due to the relatively large volume of Ba. Even for Yb and Eu, the adsorbed metal atoms are very slightly moved away from each other in the $[0\bar{1}1]$ direction but for the Ba/Si(100) surface this repulsive interaction is much larger as can be noted from the interatomic distances between the neighboring metal atoms in the (2×3) reconstruction (4.40 Å for Ba, 4.03 Å for Eu, and 3.90 Å for Yb). In the (2×1) reconstruction the metal atoms cannot be shifted in the $[0\bar{1}1]$ direction, which increases the total energy considerably on the Ba/Si(100) thus stabilizing the (2×3) reconstruction. For Eu and Yb, however, the energy gain for the formation of the (2×1) structure overcompensates the repulsive interaction between the metal atoms.

In the case of the Sm/Si(100) surface with trivalent adsorbate atoms, the (2×3) reconstruction is also close to stability for certain values of the μ_{Sm} [Fig. 7(b)]. Moreover, there are no buckled dimers for the trivalent case (the oblique symmetry leads still to the lowest total energy). Now it is found that the (2×1) surface is not semiconducting anymore thus explaining the relative stability of the (2×3) reconstruction for the trivalent atoms. This shows the importance of the valence for energetics. This result was confirmed by calculating another surface with trivalent metal atoms, namely, the Nd/Si(100) surface. The surface phase diagram is quite similar to that of the Sm/Si(100) [(2×3) is slightly more stable] and it is not shown. The energy decrease due to the oblique symmetry is of similar magnitude as for the Ba/Si, Eu/Si, and Yb/Si [0.012 eV/(1×1) area for the Nd/Si and 9 meV/(1×1) area for the Sm/Si]. There are not buckled Si dimers for the trivalent RE atoms but the average Si dimer length is decreased about 0.5% due to symmetry change, which might explain the energy decrease. It is concluded that the high stability of the (2×1) reconstruction is due to the increased degree of metal-silicon binding. In the

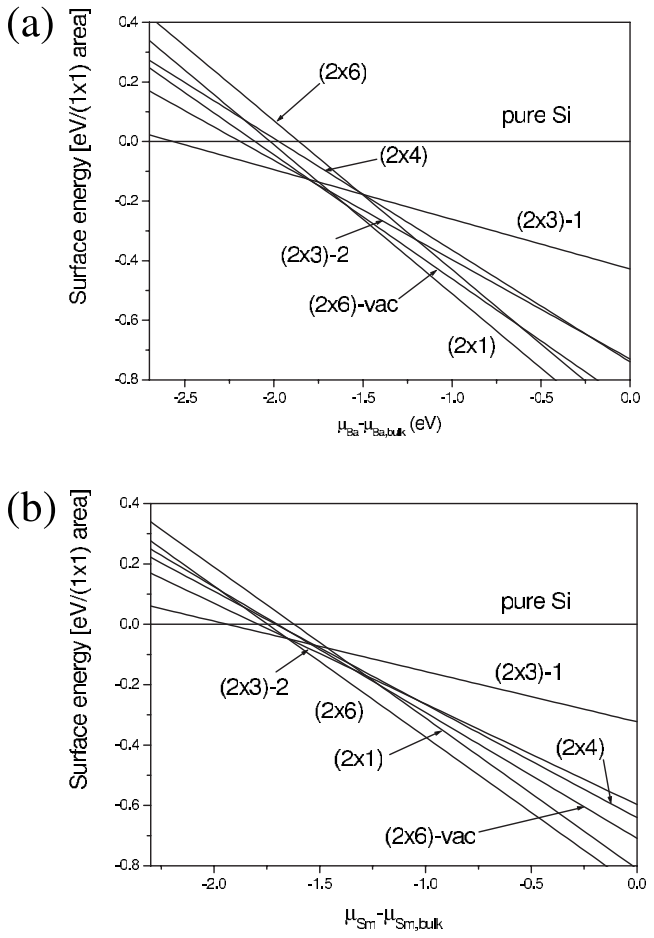

FIG. 7. Surface phase diagrams for (a) Ba/Si(100) and (b) Sm/Si(100). The atomic model for the (2×4) reconstruction is the same as the ground-state atomic model in Ref. 8. The (2×3)-1 means that there is one metal atom per (2×3) area (1/6 ML) and the (2×3)-2 that there are two metal atoms per (2×3) area (1/3 ML).

(2×3) reconstruction the dangling bonds are partly unused because there are only two metal atoms. In the (2×1) reconstruction the larger number of metal atoms allows the charge of the dangling bonds become more binding. Other factors, including the repulsive metal-metal interaction and the metallicity, can change the relative stabilities.

D. Other phases—(2×4), wavy (1×2), and (2×6) reconstructions

Here we focus on phases, which have been found in experiment and are different from the (2×1) reconstruction. It depends to a some extent on the adsorbed species, which kind of reconstructions are found in the experiments. The (2×3), (2×4), and (2×6) reconstructions have been reported for the Yb/Si(100) (Ref. 20) and Nd/Si(100) (Ref. 29), whereas Ba/Si(100) (Ref. 30), Eu/Si(100) (Ref. 31), and Sm/Si(100) (Ref. 32) showed only (2×3) and the so-called wavy (1×2) reconstruction (or a similar type for the Sm/Si). According to experimental findings, the orientation of the latter structure is rotated by 90° relative to that of the (2×1) structure and the orientation of Si dimers in the wavy (1×2) is orthogonal to that of the (2×3). It is possible that this difference is connected to different amounts of Si layers in the reconstructions. However, this peculiarity is probably not relevant for the discussion of the wavy structure in the present study because it is energetically very unfavorable for Si atoms to dimerize above the underlying Si-atom row.

Ojima *et al.*[30] proposed an atomic model for the wavy (1×2) structure on Ba/Si(100). However, this model is very unstable because the Ba atoms are supposed to locate in the cave sites, which is not energetically favorable, as found by Ciani *et al.*[7] Instead, the Ba atoms prefer valley-bridge sites. Furthermore, the Ba atoms do not tend to dimerize, as supposed in the model of Ojima *et al.* However, the (2×1) atomic model is not either the ground-state structure, instead one Ba atom per $(2\times N)$ unit cell (in which $N=3-6$) occupies a hollow position between the Si dimers.[7] Our calculations confirm these results, although the energy difference between these $(2\times N)$ and (2×1) reconstructions is very small [about 4 meV/(1×1) area for the (2×4) unit cell]. For the RE atoms considered in this study, the (2×1) reconstruction is significantly more stable than the "valley-bridge—hollow" $(2\times N)$ reconstruction. However, an atomic model should reproduce the experimental STM images reasonably and this is not the case for the $(2\times N)$ reconstruction, where the metal atom in the hollow site looks very bright and the other metal atoms rather dark (not shown) because the atom at the hollow position is in a much higher vertical position. On the other hand, in the experimental STM images for the Eu-induced wavy (1×2) structure[31] the protrusion is so large that it is impossible to associate it with an individual metal atom. Furthermore, the wavy structure corresponds to oblique lattice vectors, not rectangular lattice vectors. We calculated the valley-bridge—hollow $(2\times N)$ structure using oblique lattice vectors and $N=4$ (corresponding to a half wave of the experimental structure, i.e., U or U′ in Ref. 30, in Ref. 7 a "zigzag" structure was calculated) but the total energy is lower for the rectangular system. However, our results confirm that the wavy structure has to be closely connected to the (2×1) reconstruction with majority of the metal atoms on the valley-bridge sites. Furthermore, our calculations revealed that potentially any distortion in a metal-atom row is source of the atom height differences in the rows, and if connected to oblique lattice vectors, is prone to lead to a STM image similar to experimental STM images for the wavy structure. One potential candidate for such distortion is a vacancy in the metal-atom row. First of all, (2×3) and (2×4) reconstructions [atomic models for the (2×4) reconstruction were studied in the Ref. 8] are such structures with one vacancy. This would be also natural especially for the Ba/Si(100) in which the repulsive interaction of adsorbate atoms is rather strong. Furthermore, our findings show that a vacancy leads generally to an energy minimum with oblique lattice vectors [for the oblique (2×4) reconstruction calculations reveal one buckled Si dimer for divalent metal atoms, whereas for the rectangular (2×4) none]. The exceptions found for this trend in this study are the Ba/Si(100)(2×4) and Sm/Si(100)(2×4) reconstructions. Therefore, we also calculated a (2×6) reconstruction in which one metal atom is removed from the atomic row of the (2×1) reconstruction [labeled "(2×6)-vac" in figures].

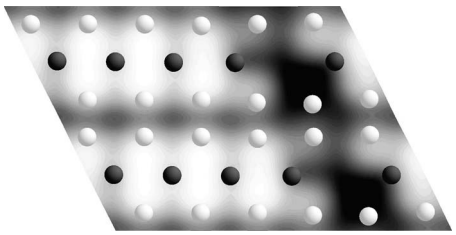

FIG. 8. Simulated STM image for the Ba/Si(100) (2×6)-vac structure with energy range of 1.4 eV below the Fermi energy. In this structure one metal atom has been removed from the metal atom row per (2×6) unit cell. The Ba atoms are shown by black spheres and the Si atoms by gray spheres. One of the Si dimers is strongly buckled.

The oblique translation vectors leading to the energy minimum are $(2a_S,a_S)$ and $(0,6a_S)$ (other oblique translation vectors were also tested). A simulated STM image for the Ba/Si(100)(2×6)-vac is shown in Fig. 8 and it can be compared to the corresponding experimental STM image in Fig. 8 in Ref. 30. The (2×6)-vac reconstruction is most stable for the Ba. The configurational entropy stabilizes it even more at finite temperatures with respect to the (2×1) reconstruction. An STM image was simulated also for a very unstable "Ojima-type" structure and this simulated image is also similar to experimental STM images for the wavy structure.

One should note that atomic models for the (2×6) reconstruction have not been suggested in literature. A careful inspection of the experimental STM images for the Yb/Si(100)(2×6) reconstruction (Figs. 6 and 9 in Ref. 20) led us to test an atomic model for the (2×6) reconstruction shown in Fig. 9. This model is equivalent to the (2×1) reconstruction, except that there is one additional Si dimer

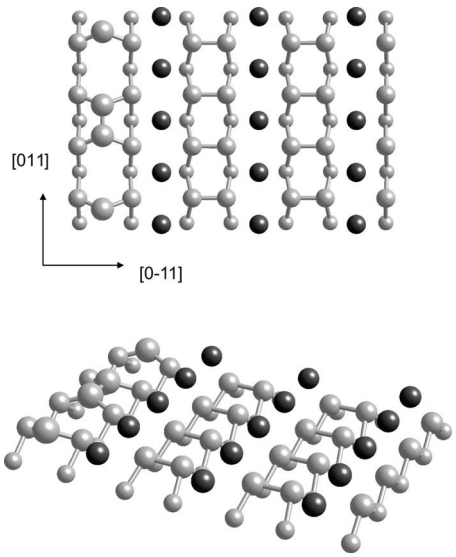

FIG. 9. Surface atomic structure (top and side views) for the atomic model of the (2×6) reconstruction proposed in this study. The one first Si layer dimer is in the same direction as the Si dimers in the (2×3) reconstruction shown in Fig. 2. The black spheres denote RE atoms and the gray spheres denote Si atoms. The first Si layer atoms are shown by larger spheres and the third Si layer atoms by smaller spheres.

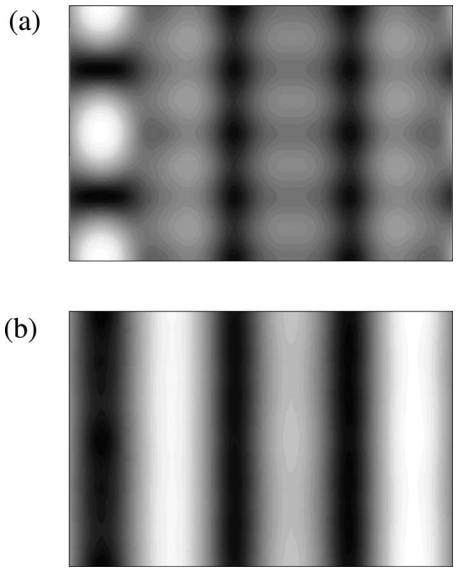

FIG. 10. Simulated STM images for the atomic model of the (2×6) reconstruction proposed in this study for energy range of (a) 2.0 eV below the Fermi energy and (b) 2.0 eV above the Fermi energy.

above the underlying full Si layer and consequently there are Si dimers in two directions. One should note, however, that the RE atom rows are in different directions in the (2×1) and (2×6) structures because the (2×6) reconstruction is obtained by removing most of the first Si layer dimers from the supercell of the (2×1) reconstruction. The RE atoms are in valley-bridge sites also in this (2×6) model. Because the RE atoms favor so much the valley-bridge site and because in the experimental STM images for the (2×6) reconstruction significant height differences were found, we considered this case, in which the first Si layer is not full. In fact, there were not many choices left to modify the structure, if the first Si layer was left intact. On the other hand, the found stripes in direction of the shorter translation vector suggest that there could be RE rows in this direction. Interestingly, this structure leads to a quite low total energy (and semiconducting state for divalent RE atoms), which is shown in phase diagrams. (Several other atomic structures were also tested but they have higher total energies.) Total energies for the (2×6) reconstruction were obtained by using the bulk value for the μ_{Si}. If the μ_{Si} is lower due to experimental conditions, the (2×6) reconstruction is stabilized even more. Especially, the (2×6) leads to lower total energy than the (2×1) for the Yb, Sm, and Nd. Furthermore, the simulated STM images (shown in Fig. 10) are in excellent agreement with the experimental images.[20,29,33] Especially, one can easily see that the images are very similar to those in Fig. 7 of Ref. 33. Therefore, we conclude that the proposed model is a prominent candidate for the atomic structure of the (2×6) reconstruction. Stress relief in the first Si layer (due to the dimerization in different directions) might stabilize the (2×6) reconstruction. On the other hand, the slight repulsion between the "additional" Si dimers and the metal atoms might destabilize this structure for the Ba/Si and Eu/Si due to the large size of the Ba and Eu atoms. There is still the

difference between Sm/Si and Nd/Si concerning experimentally found reconstructions around 1/2 ML coverage, which is not reflected in the phase diagrams. However, experimentally, the valence of the Sm can be readily intermediate between the trivalent and divalent states, and deviates from 3 + on the Sm/Si(100) surfaces,[32] which probably explains the difference (this does not affect the conclusions drawn from the calculational results for the trivalent Sm in this study).

IV. CONCLUSIONS

It has been shown that with divalent metal atoms the semiconducting state of the Si(100) surface is quite insensitive to the amount of metal atoms. This tendency is strengthened due to the possibility of Si dimer buckling, which is an important factor determining the energetics also for the divalent RE/Si(100) surfaces. Relaxation of the first Si layer affects significantly the formation of the RE/Si(100) reconstructions. In general, the oblique lattice symmetry leads to an energy minimum. When the metal atom is large enough [Ba/Si(100)], the (2×3) reconstruction can be stabilized due to the repulsive interaction of the metal atoms. With trivalent metal atoms the (2×3) is stabilized due to the loss of the semiconducting state in the competing reconstructions. It is possible that configurational entropy and kinetics stabilize the (2×3) reconstruction also for the Eu/Si and Yb/Si surfaces. Our results illustrate, how different factors control the formation of RE and Ba-induced reconstructions on the Si(100) surface, and thus we proposed the mechanisms behind the stabilization of such structures. We proposed an energetically favorable model for the (2×6) reconstruction, which leads to semiconducting state with divalent metal atoms and a good agreement with the experimental STM images. Furthermore, the character of the wavy (1×2) structure was also discussed.

ACKNOWLEDGMENTS

The calculations were performed using the facilities of the Finnish Centre for Scientific Computing (CSC) and the Mgrid project (Turku, Finland). The Swedish Research Council (L.V. and B.J.), the Swedish Foundation for Strategic Research (L.V. and B.J.), the Hungarian Scientific Research Fund (Grant No. T048827) (L.V.), the Carl Tryggers Foundation (M.P.J.P.), the Turku University Foundation (M.P.J.P.), and the Emil Aaltonen Foundation (M.P.J.P.) are also acknowledged for financial support. The financial support by the Transnational Access to the Research Infrastructure Program (TARI) is acknowledged. This work has been supported by the Academy of Finland under Grants No. 122743 (P.L.) and No. 122355 (I.J.V.) as well as Finnish Academy of Sciences and Letters (P.L.).

*Author to whom correspondence should be addressed; marko.punkkinen@utu.fi

[1] M. Kuzmin, R. E. Perälä, P. Laukkanen, and I. J. Väyrynen, Phys. Rev. B **72**, 085343 (2005), and references therein.
[2] W. C. Fan and A. Ignatiev, Surf. Sci. **253**, 297 (1991); T. Abukawa, T. Okane, and S. Kono, *ibid.* **256**, 370 (1991); A. Brodde, Th. Bertrams, and H. Neddermeyer, Phys. Rev. B **47**, 4508 (1993).
[3] A. A. Saranin, A. V. Zotov, S. V. Ryzhkov, D. A. Tsukanov, V. G. Lifshits, J. T. Ryu, O. Kubo, H. Tani, T. Harada, M. Katayama, and K. Oura, Phys. Rev. B **58**, 4972 (1998).
[4] J.-S. Kim, K.-W. Ihm, C.-C. Whang, H.-S. Kim, Y.-K. Kim, C. Lee, and C.-Y. Park, Jpn. J. Appl. Phys. **38**, 6479 (1999).
[5] A. Herrera-Gómez, P. Pianetta, D. Marshall, E. Nelson, and W. E. Spicer, Phys. Rev. B **61**, 12988 (2000).
[6] K. Ojima, M. Yoshimura, and K. Ueda, Surf. Sci. **491**, 169 (2001).
[7] A. J. Ciani, P. Sen, and I. P. Batra, Phys. Rev. B **69**, 245308 (2004).
[8] M. Kuzmin, M. P. J. Punkkinen, P. Laukkanen, R. E. Perälä, M. Ahola-Tuomi, T. Balasubramanian, and I. J. Väyrynen, Phys. Rev. B **78**, 045318 (2008).
[9] D. M. Ceperley and B. J. Alder, Phys. Rev. Lett. **45**, 566 (1980).
[10] J. P. Perdew and A. Zunger, Phys. Rev. B **23**, 5048 (1981).
[11] P. E. Blöchl, Phys. Rev. B **50**, 17953 (1994).
[12] G. Kresse and D. Joubert, Phys. Rev. B **59**, 1758 (1999).
[13] G. Kresse and J. Hafner, Phys. Rev. B **47**, 558 (1993).
[14] G. Kresse and J. Hafner, Phys. Rev. B **49**, 14251 (1994).
[15] G. Kresse and J. Furthmüller, Comput. Mater. Sci. **6**, 15 (1996).
[16] G. Kresse and J. Furthmüller, Phys. Rev. B **54**, 11169 (1996).
[17] H. J. Monkhorst and J. D. Pack, Phys. Rev. B **13**, 5188 (1976).
[18] J. Tersoff and D. R. Hamann, Phys. Rev. Lett. **50**, 1998 (1983); Phys. Rev. B **31**, 805 (1985).
[19] A. Pomyalov and Y. Manassen, Surf. Sci. **382**, 275 (1997).
[20] M. Kuzmin, R. E. Perälä, P. Laukkanen, R.-L. Vaara, M. A. Mittsev, and I. J. Väyrynen, Appl. Surf. Sci. **214**, 196 (2003).
[21] M. D. Pashley, Phys. Rev. B **40**, 10481 (1989).
[22] L. Zhang, E. G. Wang, Q. K. Xue, S. B. Zhang, and Z. Zhang, Phys. Rev. Lett. **97**, 126103 (2006).
[23] S. Yang, L. Zhang, H. Chen, E. Wang, and Z. Zhang, Phys. Rev. B **78**, 075305 (2008).
[24] E. Pehlke and M. Scheffler, Phys. Rev. Lett. **71**, 2338 (1993).
[25] A. I. Liechtenstein, V. I. Anisimov, and J. Zaanen, Phys. Rev. B **52**, R5467 (1995).
[26] J. P. Perdew, K. Burke, and M. Ernzerhof, Phys. Rev. Lett. **77**, 3865 (1996).
[27] E. Penev, P. Kratzer, and M. Scheffler, Phys. Rev. Lett. **93**, 146102 (2004).
[28] X. Hu, X. Yao, C. A. Peterson, D. Sarid, Z. Yu, J. Wang, D. S. Marshall, R. Droopad, J. A. Hallmark, and W. J. Ooms, Surf. Sci. **445**, 256 (2000).
[29] M. V. Katkov and J. Nogami, Surf. Sci. **524**, 129 (2003).
[30] K. Ojima, M. Yoshimura, and K. Ueda, Phys. Rev. B **65**, 075408 (2002).
[31] M. Kuzmin, P. Laukkanen, R. E. Perälä, R.-L. Vaara, and I. J. Väyrynen, Surf. Sci. **584**, 1 (2005).
[32] C. Ohbuchi and J. Nogami, Surf. Sci. **579**, 157 (2005).
[33] Y. Cui and J. Nogami, Surf. Sci. **603**, 3072 (2009).